NJC

Accepted Manuscript

This is an *Accepted Manuscript*, which has been through the Royal Society of Chemistry peer review process and has been accepted for publication.

Accepted Manuscripts are published online shortly after acceptance, before technical editing, formatting and proof reading. Using this free service, authors can make their results available to the community, in citable form, before we publish the edited article. We will replace this *Accepted Manuscript* with the edited and formatted *Advance Article* as soon as it is available.

You can find more information about *Accepted Manuscripts* in the Information for Authors.

Please note that technical editing may introduce minor changes to the text and/or graphics, which may alter content. The journal's standard Terms & Conditions and the Ethical guidelines still apply. In no event shall the Royal Society of Chemistry be held responsible for any errors or omissions in this *Accepted Manuscript* or any consequences arising from the use of any information it contains.

ROYAL SOCIETY OF CHEMISTRY

www.rsc.org/njc

NJC

RSCPublishing

ARTICLE

Fabrication of Fe_3O_4@Au hollow spheres with recyclable and efficient catalytic properties

Cite this: DOI: 10.1039/x0xx00000x

Qingdong Xia, Shanshan Fu, Guojuan Ren, Fang Chai, Jingjie Jiang, Fengyu Qu

Received 00th January 2012,
Accepted 00th January 2012

DOI: 10.1039/x0xx00000x

www.rsc.org/

Preparation of catalysts with superior catalytic activity, reusability and economical is highly desirable. In this work, we report a route to the facile synthesis of Fe_3O_4@Au hollow spheres. The Fe_3O_4@Au hollow spheres were prepared base on the Fe_3O_4 hollow spheres with the gold nanoparticles inlayed on their surface. The Fe_3O_4@Au hollow nanospheres were characterized by X-ray diffraction (XRD), X-ray photoelectron spectroscopy (XPS), transmission electron microscopy (TEM) and scanning electron microscopy (SEM) with energy-dispersive X-ray spectroscopy (EDX). The Fe_3O_4@Au hollow spheres exhibit remarkable catalytic activity and good reusability toward the reduction of 4-nitrophenol and potassium hexacyanoferrate (III) by $NaBH_4$ in water. In addition, the catalysts show good reusability for at least 6 successive cycles.

Introduction

Noble metal nanoparticles (NPs) have been the subject of intense research due to the unique physiochemical properties compared to their bulk counterparts and broad applications in energy conversion and storage, cancer therapy, sensing, etc., especially for catalysis.[1-6] As an important catalyst, noble metallic Au nanoparticles have been widely used in many typical pseudo-homogeneous catalysis,[7-9] such as water splitting, hydrogenation, and coupling reactions, etc. under mild reaction conditions.[10–13] However, the cost of noble metals is one of the key limitations for their practical application. One possible solution is minimum usage and reuse of the noble metal nanoparticles. To improve the efficiency and save resources, there has been an increasing trend toward the use of magnetically retrievable nanoparticles in efficient green chemical synthesis.[14] Using a catalyst containing magnetic particles allows it to be recovered and reused using an external magnet, thus avoiding the need for catalyst separation by filtration. The recovery of expensive catalysts after catalytic reactions and reusing them without loss of activity are essential features in the sustainable process development. This is primarily because these types of support display some advantageous properties, such as excellent stability, good accessibility, porosity, and the fact that tiny noble metal nanoparticles can be robustly anchored to their surfaces to provide catalytic centers. Hence, a number of efforts have been devoted to develop feasible routes for immobilizing or grafting noble metal onto magnetite supports to improve their stabilization and recycling stability. Zhao and co-workers have synthesized a kind of mesoporous Fe_3O_4@SiO_2-Au hybid composite materials with high magnetization and catalysis.[15] Ma et al. have designed a Pt nanoparticles supported on carbon coated magnetic microparticles Fe_3O_4@C@Pt as recyclable catalyst.[16] Li and Chen prepared Pt−Pd Nanoalloys supported on Fe_3O_4@C core−shell nanoparticles and used as catalyst with high catalytic activiy.[17] More recently, Vinod and co-workers reported an Au@Ni core−shell nanoparticles with synergistic catalysis.[18] Huang and Tang reported one-pot solvothermal synthesis of Au–Fe_3O_4 hybrid nanoparticles and used as reusable catalyst.[19] Otherwise, compared with the solid metal nanostructures, the hollow ones are quite distinguishable, because of their large specific surface area and high reactivity.[20–22] A specific feature of hollow sturcture is their relatively low density, particularly, hollow structures with large surface areas, which generally makes them more attractive than the corresponding core–shell particles.[23] Typically, Zhao et al. reported a one-pot process via the hydrothermal method to synthesis of Au–Fe_3O_4 hybrid hollow spheres with efficient catalysis.[24] Li and co-workers prepared a Pd based catalyst supported on amine-functionalized Fe_3O_4 hollow spheres. The Fe_3O_4@Pd afforded fast conversions for various aromatic nitro compounds under a H_2 atmosphere in ethanol even at room temperature.[25] Therefore, it is highly desirable to develop a functionalized magnetite support for immobilizing noble metal nanoparticles with hollow structure.

In this work, we prepared Au supported the Fe_3O_4 hollow spheres and used as recyclable catalyst. The fabrication

procedures for Fe_3O_4@Au hollow spheres were schematically illustrated in Scheme 1. Briefly, Fe_3O_4 hollow spheres were firstly prepared by a using a modified solvothermal method. Then Fe_3O_4 hollow spheres were modified and used as a template. The gold nanoseeds were prepared and supported on the surface of Fe_3O_4 hollow spheres by the function of $–NH_2$. The Fe_3O_4@Au hollow spheres were generated in the form of the seeded growth in situ by Au^{3+} was directly reduced on the surface of Fe_3O_4@Au nanoseeds. The gold nanoparticles were immobilized on the surface of the Fe_3O_4 nanoparticles act as a robust antenna, which could increase the area of contact with reactants. It was found that the as-prepared Fe_3O_4@Au hollow spheres exhibit an ultrahigh activity as catalysts for the reduction of 4-nitrophenol (4-NP) and potassium hexacyanoferrate (III) by $NaBH_4$.

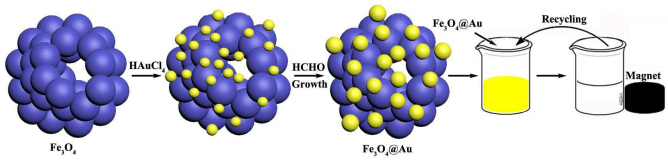

Scheme 1 View of the preparation process and the evaluation of catalysis activity Fe_3O_4@Au hollow spheres.

Experimental section

Chemicals

All chemicals used were of analytical grade or of the highest purity available. Ferric chloride hexahydrate ($FeCl_3 \cdot 6H_2O$), sodium acetate anhydrous (NaAc), potassium carbonate (K_2CO_3), trisodium citrate ($C_6H_5O_7Na_3 \cdot 2H_2O$) and formaldehyde (HCHO) were obtained from Fengchuan Chemical Company (Tianjin, China). Polyethylene glycol 2000 (PEG-2000) was purchased from Tianjin Guangfu Technology Development Co., Ltd. (Tianjin, China). Ethylence glycol (EG), ethanolamine (ETA) and ethanol was provided by Sinopharm Chemical Reagent Co., Ltd (Shanghai, China). Hydrogen tetrachloroaurate (III) trihydrate ($HAuCl_4 \cdot 3H_2O$, 99.9%), 3-aminopropyl-triethoxysilane (APTES) and sodium borohydride ($NaBH_4$, 98%) were obtained from Aladin and used as received. Potassium hexacyanoferrate (III) ($K_3Fe(CN)_6$, 99%) and 4-nitrophenol (4-NP) were supplied by Shanghai Chemical Corp. All glassware was thoroughly cleaned with freshly prepared 3:1 HCl/HNO_3 (aqua regia) and rinsed thoroughly with Mill-Q (18.2 MΩ cm^{-1} resistance) water prior to use. Mill-Q water was used to prepare all the solutions in this study.

Characterization

The morphology and size of the Fe_3O_4 hollow spheres and Au NPs were characterized by JEM-2010 (Japan) transmission electron microscope (TEM) operated at 200 kV. Scanning electron microscopy (SEM) image and energy-dispersive X-ray spec-troscopy (EDX) analysis were obtained by using a Hitachi Su-70 electron at a celeration voltage of 20 KV. X-ray powder diffraction (XRD) pattern was carried out by using a Rigaku DMax-2600 PC diffraction meter using monochromatic Cu Ka radiation. The X-ray photoelectron spectroscopy (XPS) was recorded on an Axis Ultra DLD (SHIMADZU, Japan), and the C1s line at 284.6 eV was used as the binding energy reference. Magnetic properties of the samples were measured vibrating sample magnetometer (VSM, Lake-shore 7410) at room temperature. Absorption spectra were recorded on a UV–vis spectroscopy was performed with a UV-2550 spectrophotometer (SHIMADZU, Japan) at room temperature.

Preparation of Fe_3O_4 hollow spheres

The monodisperse Fe_3O_4 hollow spheres were synthesized according to the reported literature[26,27] with slight modifications. In detail, 1.5 g of $FeCl_3 \cdot 6H_2O$ was dissolved in 40 mL of solvent containing EG (30 mL) and ETA (10 mL) to form a stable orange solution. 4.0 g of NaAc and 1.0 g PEG-2000 were added into the above solution under vigorously magnetic stirring until completely dissolved. The homogeneous solution obtained was transferred to a Teflon-lined stainless-steel autoclave (50 mL), sealed and heated at 200°C for 8 h. After the reaction, the autoclave was cooled to ambient temperature naturally, and the solid products were collected by applying a magnet, and were washed with water and ethanol several times. The products were dried under vacuum at 60 °C for 12 h.

APTES-Modified Fe_3O_4 hollow spheres

The Fe_3O_4 hollow spheres should modified by APTES to stabilize the resultant Au nanoseed. According to the reported literature,[15,28] the 100 mg of Fe_3O_4 hollow nanospheres was dispersed into 40 mL ethanol, and then the suspension was ultrasonicated for at least 20 min to ensure uniform dispersion of the magnetic Fe_3O_4 hollow nanospheres. Then, 400 uL APTES was added into the suspension with continuous mechanical stirring 3 h at room temperature. Finally, with the help of a magnet, the APTES-modified Fe_3O_4 hollow nanospheres were harvested and repeatedly washed with ethanol and deionized water, and redispersed in water (50 mL) to form a homogeneous dispersion.

Synthesis of Fe_3O_4@Au nanoseeds and Fe_3O_4@Au hollow spheres

Firstly, the gold nanoseeds were 3.5 nm prepared by using the $NaBH_4$ as reduction.[29] Typically, a 20 mL aqueous solution containing 2.5×10^{-4} M $HAuCl_4$ and 2.5×10^{-4} M trisodium citrate was prepared in a conical flask. Next, 0.6 mL of ice-cold, freshly prepared 0.1 M $NaBH_4$ solution was added to the solution while stirring. The solution turned pink immediately after adding $NaBH_4$, indicating particle formation and for further uses. For preparation of Fe_3O_4@Au nanoseeds,[30] 30 mL of the Au nanoparticle solution was mixed with 50 mL of aqueous dispersion of APTES-Fe_3O_4 hollow nanospheres by quick ultrasonication in a water bath. The mixture was subjected to mechanical stirring for 2 h, and the Fe_3O_4@Au nanoseeds were collected with a magnet, washed with ethanol

and deionized water 3 times and redispersed in water (5 mL) to form a homogeneous dispersion.

In order to grow the gold nanoparticles on the surface of Fe_3O_4 hollow spheres,[31] 1.5 ml of 1% $HAuCl_4$ solution was added to 100 ml of 2 mM potassium carbonate aqueous solution, under stirring vigorously for 30 min, the yellow colored solution became colorless gradually. The solution aged over night to form $Au(OH)_4^-$ ions in a refrigerator at 4℃. At the Au growth step, Fe_3O_4@Au nanoseeds solution were added into 20 mL of gold hydroxide solution, and then 80 uL formaldehyde was added to the solution while mechanical stirring. The bigger gold nanoparticles formed in situ based on Au nanoseeds the surface of the Fe_3O_4 hollow spheres. Finally, the Fe_3O_4@Au hollow spheres were separated with a magnet and washed with deionized water and dried in vacuum at 50℃ 6 h.

Catalytic reduction of 4-nitrophenol (4-NP)

The catalytic properties of Fe_3O_4@Au hollow spheres were systematically examined by two experiments the reduction of 4-NP[32] and $K_3Fe(CN)_6$.[33] For catalytic reduction of 4-NP, aqueous solutions of 4-NP (0.01 M, 0.03 mL) and freshly prepared aqueous $NaBH_4$ solution (0.5 M, 0.2 mL) were mixed with water (2.5 mL) in a quartz cuvette without stirring. Then the Fe_3O_4@Au hollow spheres aqueous suspension (25 μL, 2.8 $mg \cdot mL^{-1}$) was injected without any stirring. The reaction was monitored by taking absorption spectra. To further test the reusability of the catalysts, the used Fe_3O_4@Au hollow spheres were separated from the solution with a magnet for next cycle of catalytic reaction after the reduction process was complete. Similar to the above mentioned procedure was repeated 6 times. In order to ensure the quantity of catalyst was enough to centrifuge in the process of recycle, the 100 μL, 2.8 $mg \cdot mL^{-1}$ of Fe_3O_4@Au hollow spheres was added in reaction solution.

Catalytic reduction of $K_3Fe(CN)_6$.

The reduction of $K_3Fe(CN)_6$ was also performed in a quartz cuvette and monitored using UV-vis spectroscopy at room temperature.[33,34] The reduction of $K_3Fe(CN)_6$ was carried out according to a typical reaction, 0.4 mL of 8×10^{-3} M $K_3Fe(CN)_6$ was added in 1.2 mL deionized water, then the 25 μL, 2.8 $mg \cdot mL^{-1}$ of Fe_3O_4@Au hollow spheres was added, followed by the rapid addition of 0.8 mL of 0.040 M ice-cold fresh $NaBH_4$ solution. To further investigate the reusability of the Fe_3O_4@Au hollow spheres as catalysts, the used Fe_3O_4@Au hollow spheres was separated from the solution with a magnet after the whole reduction process was complete. In order to ensure the quantity of catalyst was enough to separate and reuse in the process of recycle, the 100 μL, 2.8 $mg \cdot mL^{-1}$ of Fe_3O_4@Au hollow spheres was added in reaction solution. Similar to the above reduction process was recycled 12 times.

Results and discussion

Representative transmission electron microscopy (TEM) images were recorded to exam the morphology, size and hollow structure of magnetic Fe_3O_4 hollow spheres, Fe_3O_4@Au nanoseeds, and Fe_3O_4@Au hollow spheres. As shown in Fig. 1a, the diameter of the as-synthesized Fe_3O_4 hollow spheres was between 100-120 nm. The Fe_3O_4 hollow spheres were performed by many nanoparticles with diameter about 25-30 nm. The hollow hole of the Fe_3O_4 spherical structure can be seen clealy from the magnified image showed in the inset. The Fe_3O_4@Au nanoseeds can be observed in the Fig. 1b, which indicated many Au nanoseeds with diameter of 3.5 nm were stuck on the surface of the Fe_3O_4 hollow spheres. And the nanoseeds can be observed inlayed in the inwall of Fe_3O_4 hollow spheres from the enlarged image of inset. After the growth of Au nanoseeds, the surface of hollow spheres was relatively rough, which indicated that they were composed of tiny primary nanoparticles. The diameter of gold nanoparticles was up to around 6 nm, which were indicated in the Fig. 1c. Meanwhile, from Fig. 1d, which is magnified from Fig. 1c, it can also be concluded that the gold nanoparticle size distribution (Fig. S1) was centred 6 nm. The hollow structures were filled with the gold nanoparticles which can be seen in the enlarged image (Fig. 1d).

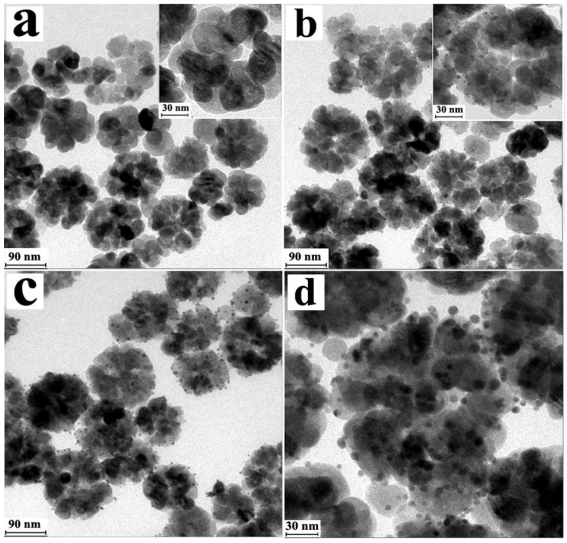

Fig. 1 TEM images of (a) Fe_3O_4 hollow spheres, (b) Fe_3O_4@Au nanoseeds, (c) Fe_3O_4@Au hollow spheres and (d) magnified image of (c).

The SEM analysis was also performed to confirm the shape, morphology and internal structure of Fe_3O_4 hollow spheres, Fe_3O_4@Au nanoseeds and Fe_3O_4@Au hollow spheres for detailed investigation of final product. From the SEM of Fe_3O_4 hollow spheres (Fig. 2a), Fe_3O_4 hollow spheres with a uniform and non-aggregated nature revealed a relatively coarse surface and a mean diameter of ~100 nm, and composed of small primary nanoparticles with an average size of 25–30 nm. And the obvious hollow hole can be observed in the Fe_3O_4 spheres which was consistent with the TEM. The Fig. 2b and 2c indicated the small Au nanoseeds and Au NPs were supported on the surface of Fe_3O_4 hollow spheres, which was also consistent with TEM. From the SEM, it can be deduced that the amount of loaded of Au was much less than the reported structure.[21] Fig. 2d shows a typical EDX spectrum of the Fe_3O_4@Au

hollow spheres, which indicates the existence of Au, Fe and O. Other signals in the EDX spectrum arise from silicon slice. The amount of Au NPs in the Fe_3O_4@Au hollow spheres was 2.54 % tested by ICP measurement, which was less amount compared to the reported similar structure.[17,24,31] The result was consistent with the EDX spectrum. Owing to the less expensive noble metal materials, the method of synthesis of Fe_3O_4@Au hollow spheres was economical. The nitrogen adsorption desorption isotherms of three materials (Fig. S2) were recorded and the BET surface area were calcined 41.71 m^2/g, 42.67 m^2/g and 37.57 m^2/g, respectively.

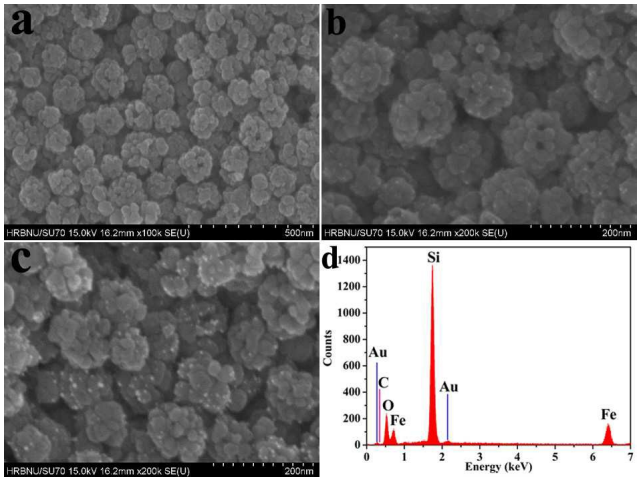

Fig. 2 SEM images of (a) Fe_3O_4 hollow spheres, (b) Fe_3O_4@Au nanoseeds, (c) Fe_3O_4@Au hollow spheres, and (d) EDX spectrum analysis of (C).

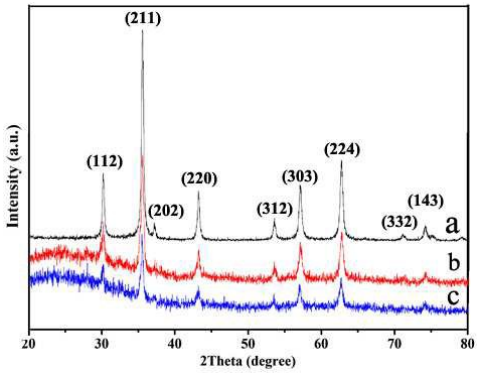

Fig. 3 XRD patterns of (a) Fe_3O_4 hollow spheres, (b) Fe_3O_4@Au nanoseeds, (c) Fe_3O_4@Au hollow spheres.

Figure 3 shows diffraction signals of Fe_3O_4, Fe_3O_4@Au nanoseeds and Fe_3O_4@Au hollow spheres in XRD analysis. The sharp diffraction peaks were indexed to (112), (211), (202), (220), (312), (303), (224), (332) and (143) Bragg reflection of crystalline cubic inverse spinel of bulk Fe_3O_4, respectively (JCPDS no. 75-1609).[26] Due to the high dispersity and low loading of Au, there is no the obvious characteristic Au peaks emerged in the diffraction pattern of Fe_3O_4@Au nanoseeds and Fe_3O_4@Au hollow spheres. The presence of Au can be proved by the EDX and ICP measurement.

The XPS was performed to investigate the electronic state of Au on the surface of the Fe_3O_4@Au hollow spheres. The XPS survey spectrum of Fe_3O_4@Au hollow spheres showed peaks due to C_{1s} (284.6 eV), O_{1s} (532.6 eV) and Au_{4f}(84.0 eV). As shown in Fig. 4, the high-resolution XPS Au 4f spectrum displayed two peaks corresponding to $4f_{7/2}$ and $4f_{5/2}$ doublet at 83.4 and 86.95 eV, respectively. The XPS binding energy of Au $4f_{7/2}$ was consistent with zerovalent Au.[35]

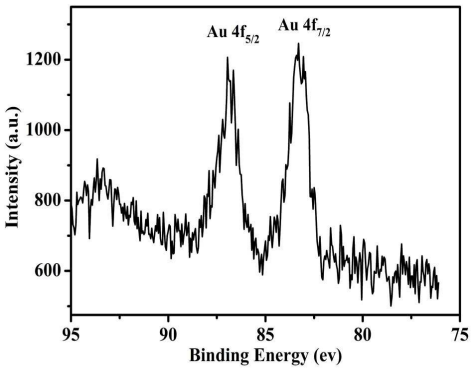

Fig. 4 High-resolution XPS of Au_{4f} spectrum of Fe_3O_4@Au hollow spheres.

In our experiments, fresh prepared Fe_3O_4@Au hollow spheres showed its strong magnetic property and can be easily collected using a permanent magnet (inset of Fig. 5). In order to quantify the magnetism and make sure whether the Fe_3O_4@Au hollow spheres would bring serious decay in their magnetism, the magnetic hysteresis loop was measured by a vibrating sample magnetometer. As illustrated in Fig. 5, all of the samples were superparamagnetic and both the remanent magnetizations and coercivities were closed to zero. The magnetization saturation value of the Fe_3O_4 hollow spheres was 84.93 emu/g. After modified the gold nanoseeds and growth in the Au^{3+}, the magnetization saturation value of Fe_3O_4@Au nanoseeds and Fe_3O_4@Au hollow spheres were 81.23 emu/g and 76.36 emu/g, respectively. As a result, the decoration of gold nanoseeds and the further growth of gold nanoparticles could weaken the magnetic saturation value of the sample. However, the magnetic saturation value of the Fe_3O_4@Au nanoseeds and Fe_3O_4@Au hollow spheres still remained at a high level which possesses a magnetic saturation value of 89.9% of fresh prepared Fe_3O_4 hollow spheres. Therefore, the magnetic actuation of the Fe_3O_4 hollow spheres was feasible.

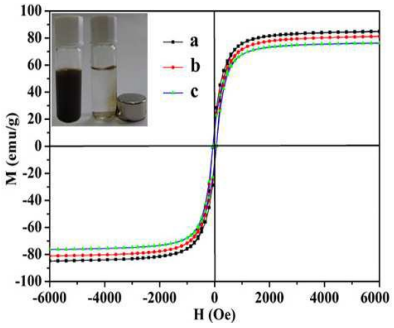

Fig. 5 Magnetization curves of the (a) Fe_3O_4 hollow spheres, (b) Fe_3O_4@Au nanoseeds, (c) Fe_3O_4@Au hollow spheres. The insets show their suspensions before and after magnetic separation by an external magnet.

Catalysis

Among the transition metal-catalyzed redox reactions, the reduction of nitroaromatics is one of the most crucial ones. Noble metal nanoparticle catalysts are widely employed for the reduction of 4-NP to 4-AP.[31,32] Catalytic reduction of 4-NP by borohydride ions (BH_4^-) in the presence of a metal catalyst has become one of the model reactions for evaluating the catalytic activity of noble metallic nanoparticles. In order to test the catalysis of the Fe_3O_4@Au nanoseeds and Fe_3O_4@Au hollow spheres, the reactions of reduction of 4-NP were performed at the same condition. The equal quantity of different catalyst was added into the reaction pool, the whole reaction can be monitored spectroscopically. Although the reaction is thermodynamically, without catalyst, no reaction occurred after the addition of the freshly-prepared $NaBH_4$ solution. After addition of a small amount of the catalyst (Fe_3O_4@Au nanoseeds and Fe_3O_4@Au hollow spheres), the 4-NP was reduced to 4-AP by $NaBH_4$ with the change of color of solution. 4-NP showed a distinct spectral profile with an absorption maximum at 317 in neutral or acidic solution which can be detected in Fig. S3. The addition of $NaBH_4$ deprotonates the OH group of 4-NP, and the absorption peak shifts to 400 nm immediately (Fig. S3), which is due to the formation of 4-nitrophenolate ion.[29,30] In order to estimate the efficiency of the catalyst, the predetermined calibration curve has been confirmed in Fig. S4. The reduction kinetics was monitored by UV-vis absorption spectroscopy of the reaction mixture after the addition of the catalyst. When the reduction of 4-NP is started, the absorption peak at 400 nm gradually decreases in intensity. Meanwhile, a small shoulder at 300 nm gradually rises, which is attributed to absorption of 4-AP. As observed, the reduction of 4-NP to 4-AP was finished within 200 s using the Fe_3O_4@Au hollow spheres as the catalyst (Fig. 6c), which was much shorter than that of the as-prepared Fe_3O_4@Au nanoseeds (400 s, Fig. 6a). The catalytic reduction of 4-NP can generally be considered to be the pseudo-first-order reactions in regard to the reactant alone on the basis of the almost unchanged concentration of $NaBH_4$ during catalysis, since the concentration of $NaBH_4$ was much higher than that of 4-NP. The reaction rate constant k is calculated from the slope of the linear section of the plots of $\ln(C_t/C_0)$ versus t (Fig. 6b and 6d).[36] Compared with the as-prepared Fe_3O_4@Au nanoseeds (k: $9.99\times10^{-3}\cdot s^{-1}$), the Fe_3O_4@Au hollow spheres exhibit a better catalytic activity for the 4-AP reduction (k: $20.15\times10^{-3}\cdot s^{-1}$). Remarkably, the k value is also higher than those of the Au–Fe_3O_4 hybrid nanoparticles, Fe_3O_4@Au core shell and so on (Table S1). The results indicated that Fe_3O_4@ Au hollow spheres was a good catalyst with high efficiency.

Because the reusability of the catalyst was one important issue for practical applications, the reusability of Fe_3O_4@Au hollow spheres was tested in detail (Fig. 7 and Fig. S5). To further test the reusability of the catalysts, six successive cycles of catalytic reduction were carried out with the Fe_3O_4@Au hollow spheres. According to the UV-vis spectra of reduction (Fig. S5), the kinetic rate were calculated to $35.66\times10^{-3}\cdot s^{-1}$, $8.6\times10^{-3}\cdot s^{-1}$, $5.34\times10^{-3}\cdot s^{-1}$, $4.48\times10^{-3}\cdot s^{-1}$, $3.65\times10^{-3}\cdot s^{-1}$ and $2.88\times10^{-3}\cdot s^{-1}$, respectively. The catalysts can be successfully recycled and reused for at least six successive cycles of reaction with a stable conversion efficiency of around 100%. Through the above analysis, it is concluded that the Fe_3O_4@Au hollow spheres have excellent catalytic activity for the reduction of 4-NP, which may be attributed to the synergistic effect between Au and Fe_3O_4 nanoparticles and the rich edges and corner atoms derived from the Au NPs on the surface of hollow spheres.[24] Otherwise, The hollow structure of the catalyst was active for the catalytic reaction, which is mainly due to the hollow structure were composed of the small Fe_3O_4 NPs with Au NPs, so as to improve the catalysis efficiency. The Fe_3O_4@Au hollow spheres were well-dispersed and exposed inside and outside surface of gold nanoparticle, allowing effective contact between the reactants with catalyst of the reaction. Thus, the Fe_3O_4@Au hollow spheres exhibited a good reusable catalytic activity.

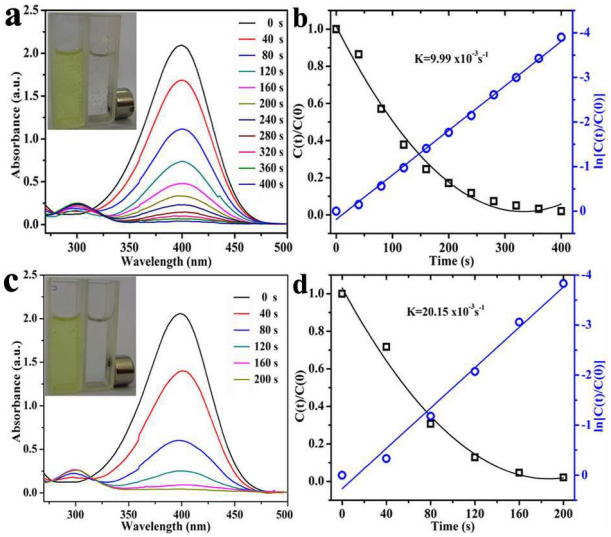

Fig. 6 UV-vis spectra and kinetic rate of the reduction of 4-NP by $NaBH_4$ in the presence of Fe_3O_4@Au nanoseeds (a, b) and Fe_3O_4@Au hollow spheres (c, d). The inset pattern is a photograph of change the color of the solution before and after reaction and the magnetic separation.

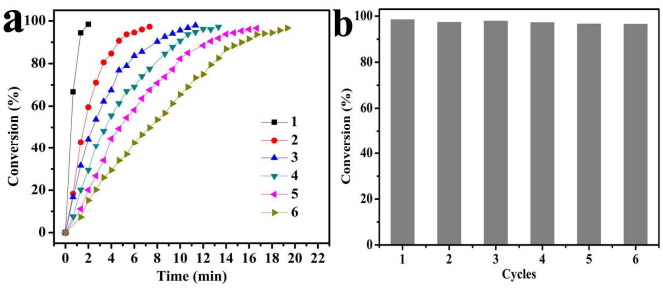

Fig. 7 (a) Relationship of the conversion (%) of 4-NP and the reaction time over Fe_3O_4@Au hollow spheres catalysts after 1-6 reused, respectively. (b) the reusability of Fe_3O_4@Au hollow spheres as a catalyst for the reduction of 4-NP with $NaBH_4$.

In order to evaluate the stability of the materials in the reaction of catalysis, the SEM and EDX of the catalyst after

reused 1, 3, 6 times were recorded and showed in the Fig. S6. As can be seen in the SEM images (Fig. S6a), the structure and morphology of the Fe_3O_4@Au hollow spheres after used 1 cycle has no obvious change compared with the Fig. 2c. After 3 recycles, though the Fe_3O_4@Au hollow spheres still remained the group of orbicular nanospheres, the little gold nanoparticles could not be found from the surface of the Fe_3O_4 hollow spheres (Fig. S6b). When the reaction was recycled 6 times, the hollow structure of Fe_3O_4@Au hollow spheres collapsed (Fig. S6c). Accompanied the process of reaction, deduced from EDX reports, the components of Au and Fe increased gradually due to the collapsed of the structure. After recycled six times, as catalyst, the Fe_3O_4@Au hollow spheres still kept the catalytic activity. The seventh reaction of catalysis has been studied, and the 4-NP can be degraded completely (Fig. S7), and the kinetic rate K was calculated to $1.97\times10^{-3}\cdot s^{-1}$. So, the above results indicated that the catalyst show good reusability for at least 6 successive cycles.

Since the $K_3Fe(CN)_6$ reduction was considered as a model electron-transfer reaction, to further study the catalytic properties, the reduction of $K_3Fe(CN)_6$ with $NaBH_4$ was selected for monitoring the catalytic activity of Fe_3O_4@Au towards an inorganic reaction. The light yellow aqueous $K_3Fe(CN)_6$ solution shows absorption at 420 nm. After the addition of $NaBH_4$, the intensity of absorption can decrease gradually due to the formation of $K_4Fe(CN)_6$ within 12 h (Fig. S8). However, after the addition of 25 μL of catalyst, the absorption peak at 420 nm significant decreased and the reaction process totally completed within 240s and 150s, respectively. UV-vis investigations demonstrate that the catalytic activity of Fe_3O_4@Au hollow spheres was also better than that of the as-prepared Fe_3O_4@Au nanoseeds (Fig. 8), indicating that Fe_3O_4@Au hollow spheres have also excellent catalytic activity for the reduction of the $K_3Fe(CN)_6$.[35] In all runs, the concentration of $NaBH_4$ was chosen to exceed the concentration of hexacyanoferrate(III). In this way, the kinetics of the reduction process can be treated as a pseudo-first-order reaction in hexacyanoferrate.[22] The reaction rate constant k is calculated from the slope of the linear section of the plots of $\ln(C_t/C_0)$ versus t (inset of Fig. 8a and 8b), $18.65\times10^{-3}\cdot s^{-1}$ and $36.55\times10^{-3}\cdot s^{-1}$ respectively. Compared with the reported work,[23,33,34] the Fe_3O_4@Au hollow spheres exhibited a better catalytic activity. The results indicated the high catalytic activity of Fe_3O_4@Au toward the reduction of $[Fe(CN)_6]^{3-}$ to $[Fe(CN)_6]^{4-}$ ions.

Though the size of nanoseeds were much little than the gold nanoparticle, however, compared in two process of catalysis, the Fe_3O_4@Au hollow sphere was a better catalyst. From the BET of these two catalysts, there is little difference in comparison. But the amount of gold nanoseeds and gold nanoparticles supported on the Fe_3O_4 were calculated to 1.034×10^{-3} mg and 1.778×10^{-3} mg in the process of catalysis. So, most possible reason was the amount of gold supported on the Fe_3O_4@Au hollow spheres was much higher than nanoseeds.

To further test the reusability in reduction of $K_3Fe(CN)_6$, twelve successive cycles of catalytic reduction were carried out with the Fe_3O_4@Au hollow spheres as catalyst. As can be seen in the Fig. 9, the catalyst can be reused at the end of the reaction, but the effect of the recovered catalyst on the reaction time of subsequent reaction is depressed gradually from 150 s to a 690 s after 10 cycles, and a maximum of 1170 s after 12 cycles (Fig. 9 and Fig. S9). Using an external magnetic field, the catalyst can be easily recycled, and long-life and high reusability are demonstrated without visible decrease in the catalytic performance after running even for more than 12 times. As expected, linear correlation of $\ln(C_t/C_0)$ versus t of the all runs were obtained and indicated in the Fig. S9. The kinetic constant k was up to $54.01\times10^{-3}\cdot s^{-1}$ in first cycle, $15.61\times10^{-3}\cdot s^{-1}$ after 6 cycles, and $2.75\times10^{-3}\cdot s^{-1}$ after 12 turns, which was higher than that for other Au catalyst.[34] All above results indicated that the Fe_3O_4@Au hollow spheres can be used as a recyclable and efficient catalyst.

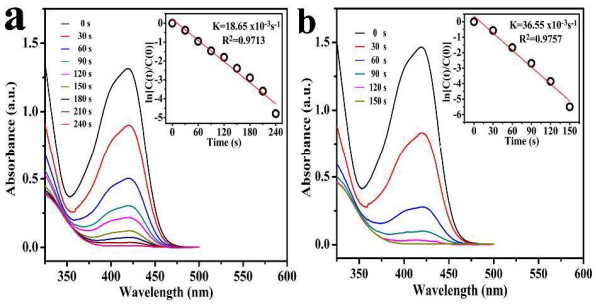

Fig. 8 UV-vis spectra and kinetic rate of the reduction of $K_3Fe(CN)_6$ by $NaBH_4$ in the presence of (a) Fe_3O_4@Au nanoseeds and (b) Fe_3O_4@Au hollow spheres.

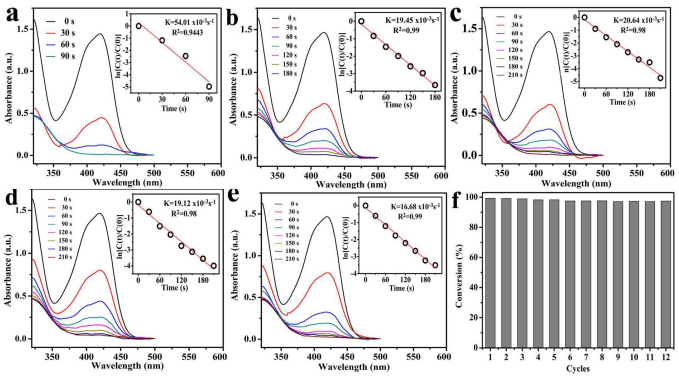

Fig. 9 The UV–vis spectra and kinetic rate of reduction of $K_3Fe(CN)_6$ by $NaBH_4$ under the catalysis of Fe_3O_4@Au for 1-5 times (a-e), the rate constant k is 54.01×10^{-3}, 19.45×10^{-3}, 20.64×10^{-3}, 19.12×10^{-3}, and $16.68\times10^{-3}\cdot s^{-1}$, respectively. (f) The reusability of Fe_3O_4@Au hollow spheres as a catalyst for the reduction of $K_3Fe(CN)_6$ with $NaBH_4$.

Conclusion

We have demonstrated a facile synthesis of Fe_3O_4@Au hollow spheres and confirmed that the Fe_3O_4@Au hollow spheres. The preparation of Fe_3O_4@Au was economical due to the amount of loading was much less. Due to the hollow structure provided large specific surface area with high reactivity, the as-prepared

Fe_3O_4@Au catalysts exhibited an excellent activity for catalytic reduction of 4-NP and $K_3Fe(CN)_6$ by $NaBH_4$. Owing to incorporation of Fe_3O_4 nanoparticles, the catalysts could be quickly recycled by magnet, and hence they exhibited good reusability. We also anticipate that Fe_3O_4@Au hollow spheres may provide a platform for broad potential in reduction of Ag, Pt and Pd, and will be useful for discovering low-cost, highly efficient catalysts for industrially important chemical reactions.

Acknowledgements

The authors gratefully acknowledge financial support from the National Natural Science Foundation of China (21205024), the National Science Foundation for Post-doctoral Scientists of China (2012M520659, 2013T60307), the Natural Science Foundation of Heilongjiang Province (B201305), the Harbin Science and Technology bureau (2014RFQXJ151) and Program for Scientific and Technological Innovation Team Construction in Universities of Heilongjiang (2011TD010).

Notes and references

Key Laboratory for Photonic and Electronic Bandgap Materials, Ministry of Education, Harbin Normal University, Harbin 150025, P. R. China. E-mail: fangchai@gmail.com, jiangjingjie80@163.com, qufengyuchem@hrbnu.edu.cn

† Electronic Supplementary Information (ESI) available. See DOI: 10.1039/b000000x/

1 N. L. Rosi and C. A. Mirkin, *Chem. Rev.*, 2005, **105**, 1547–1562.
2 P. K. Jain, X. Huang, I. H. El-Sayed and M. A. El-Sayed, *Acc. Chem. Res.* 2008, **41**, 1578–1586.
3 Y. G. Guo, J. S. Hu and L. J. Wan, *Adv. Mater.*, 2008, **20**, 2878–2887.
4 H. Zhang, M. Jin and Y. Xia, *Chem. Soc. Rev.*, 2012, **41**, 8035–8049.
5 C. Gao, Z. Lu, Y. Liu, Q. Zhang, M. Chi, Q. Cheng and Y. Yin, *Angew. Chem. Int. Ed.*, 2012, **51**, 5629–5633.
6 A. M. Alkilany, S. E. Lohse and C. J. Murphy, *Acc. Chem. Res.*, 2013, **46**, 650–661.
7 M. C. Daniel and D. Astruc, *Chem. Rev.*, 2004, **104**, 293–346.
8 M. Rudolph and A. S. Hashmi, *Chem. Soc. Rev.*, 2012, **41**, 2448–2462.
9 D. T. Thompson, *Nano Today*, 2007, **2**, 40–43.
10 K. Maeda, K. Teramura, D. Lu, N. Saito, Y. Inoue and K. Domen, *Angew. Chem., Int. Ed.*, 2006, **45**, 7806–7809.
11 J. E. Mondloch, X. Yan and R. G. Finke, *J. Am. Chem. Soc.*, 2009, **131**, 6389–6396.
12 S. Wu, J. Dzubiella, J. Kaiser, M. Drechsler, X. Guo, M. Ballauff and Y. Lu, *Angew. Chem., Int. Ed.*, 2012, **51**, 2229–2233.
13 A. Corma and P. Serna, *Science*, 2006, **313**, 332–334.
14 M. Xie, F. W. Zhang, Y. Long and J. T. Ma, *RSC Adv.*, 2013, **3**, 10329–10334
15 Y. H. Deng, Y. Cai, Z. K. Sun, J. Liu, C. Liu, J. Wei, W. Li, C. Liu, Y. Wang and D. Y. Zhao, *J. Am. Chem. Soc.*, 2010, **132**, 8466–8473.
16 M. Xie, F. W. Zhang, Y. Long and J. T. Ma, *RSC Adv.*, 2013, **3**, 10329–10334.
17 P. Zhang, R. Li, Y. M. Huang and Q. W. Chen, *ACS Appl. Mater. Interfaces*, 2014, **6**, 2671−2678.
18 A. B. Vysakh, C. L. Babu and C. P. Vinod, *J. Phys. Chem. C*, 2015, **119**, 8138-8146.
19 X. W. Meng, B. Li, X. L. Ren, L. F. Tan, Z. B. Huang and F. Q. Tang, *J. Mater. Chem. A*, 2013, **1**, 10513–10517.
20 X. Guo, W. Ye, H. Y. Sun, Q. Zhang and J. Yang, *Nanoscale*, 2013, **5**, 12582–12588.
21 L. Gao, J. Fei, J. Zhao, H. Li, Y. Cui and J. Li, *ACS Nano*, 2012, **6**, 8030–8040.
22 H. Liu, J. Qu, Y. Chen, J. Li, F. Ye, J. Y. Lee and J. Yang, *J. Am. Chem. Soc.*, 2012, **134**, 11602–11610.
23 I. Pastoriza-Santos, J. Pérez-Juste, S. Carregal-Romero, P. Hervés and L. M. Liz-Marzán, *Chem. Asian J.*, 2006, **1**, 730–736.
24 Q. Gao, A. W. Zhao, H. Y. Guo, X. C. Chen, Z. B Gan, W. Y. Tao, M. F. Zhang, R. Wu and Z. X. Li, *Dalton Trans.*, 2014, **43**, 7998–8006.
25 P. Wang, H. X. Zhu, M. M. Liu, J. R. Niu, B. Yuan, R. Li and J. T. Ma, *RSC Adv.*, 2014, **4**, 28922–28927.
26 Y. C. Zhu, J. Lei and Y. Tian, *Dalton Trans.*, 2014, **43**, 7275–7281.
27 H. Deng, X. Li, Q. Peng, X. Wang, J. Chen and Y. Li, *Angew. Chem., Int. Ed.*, 2005, **44**, 2782–2785.
28 X. M. Zhang, S. S. Ye, X. Zhang and L. P. Wu, *J. Mater. Chem. C*, 2015, **3**, 2282–2290.
29 N. R. Jana, L. Gearheart and C. J. Murphy, *Langmuir*, 2011, **17**, 6782–6786.
30 S. N. Abdollahi, M. Naderi and G. Amoabediny, *Colloids and Surfaces A*, 2013, **436**, 1069–1075.
31 Z. U. Rahman, Y. H. Ma, J. Hu, Y. Y. Xu, W. F. Wang and X. G. Chen, *RSC Adv.*, 2014, **4**, 5012–5020.
32 Z. Jin, M. Xiao, Z. H. Bao, P. Wang and J. F. Wang, *Angew. Chem. Int. Ed.*, 2012, **51**, 6406–6410.
33 X. M. Miao, T. T. Wang, F. Chai, X. L. Zhang, C. G. Wang and W. D. Sun, *Nanoscale*, 2011, **3**, 1189–1194.
34 D. Y. Du, J. S. Qin, T. T. Wang, S. L. Li, Z. M. Su, K. Z. Shao, Y. Q. Lan, X. L. Wang and E. B. Wang, *Chem. Sci.*, 2012, **3**, 705–710.
35 H. L. Yang, S. W. Li, X. Y. Zhang, X. Y. Wang and J. T Ma, *J. Mater. Chem. A*, 2014, **2**, 12060–12067.
36 R. P. Zhao, M. X. Gong, H. M. Zhu, Y. Chen, Y. W. Tang and T. H. Lu, *Nanoscale*, 2014, 6, 9273–9278.

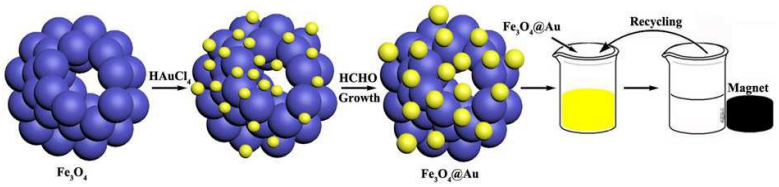

View of the preparation process and the evaluation of catalysis activity Fe_3O_4@Au hollow spheres.